



Fabrication of graphene nanoribbon-based enzyme-free electrochemical sensor for the sensitive and selective analysis of rutin in tablets

Ningappa Kumara Swamy^{1,2} · Kikkeri Narasimha Shetty Mohana¹ · Mahesh Bhaskar Hegde¹ · Ambale Murthy Madhusudana¹ · Kamalraj Rajitha¹ · Saurav Ramesh Nayak¹

Received: 14 November 2020 / Accepted: 10 March 2021 / Published online: 5 April 2021
© The Author(s), under exclusive licence to Springer Nature B.V. 2021

Abstract

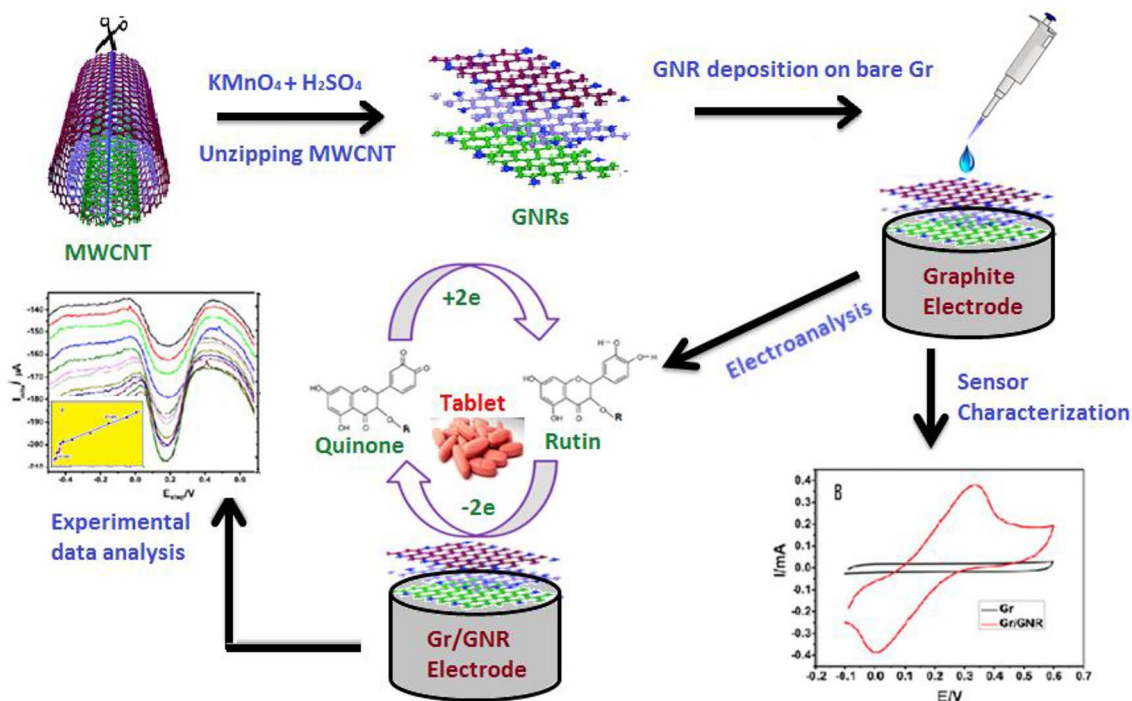
Graphene nanoribbon (GNR) is a potential sensor material owing to its high surface area, high aspect ratio, variable band gap, and high density of reactive edges. Herein, for the first time, we propose a binder-free and non-enzymatic sensor for the detection and electro-analysis of rutin using GNRs. GNRs were first synthesized from multi-walled carbon nanotubes (MWCNTs) by chemical unzipping in an oxidative environment and later casted onto graphite (Gr) electrode to get Gr/GNRs sensor. The developed sensor exhibited excellent electrocatalytic activity towards oxidation of rutin in phosphate-buffered solution (PBS) with a pair of well-defined redox peaks for rutin. Cyclic voltammetry (CV) studies showed linear dependence of sensor response on the scan rate ($R^2=0.992$) and the electrode reaction occurred via diffusion-controlled charge transfer mechanism. Differential pulse voltammetry (DPV) measurements showed the existence of linear correlation between sensor response and the concentration of rutin with a detection limit of (LOD) 7.862 nM and sensitivity of 917.23 $\mu\text{A } \mu\text{M}^{-1} \text{ cm}^{-2}$. Further, the sensor showed good stability and selectivity which are attributed to synergic effects of GNRs as a sensing material. The proposed sensor was tested for its practical applicability by successfully analyzing rutin content in pharmaceutical rutin tablets which suggest that the proposed sensor can find application in the analysis of rutin in food, drug tablets, and nutraceutical samples.

✉ Kikkeri Narasimha Shetty Mohana
drknmohana@gmail.com

¹ Department of Studies in Chemistry, University of Mysore,
Mysuru, Karnataka 570006, India

² Department of Chemistry, JSS Science and Technology
University, Mysuru, Karnataka 570006, India

Graphic abstract



Graphical Abstract: Schematic view of fabrication of rutin sensor using MWCNT derived GNRs

Keywords Graphene nanoribbon · Multiwalled carbon nanotube · Rutin sensor · Electroanalyst · Rutin tablet

1 Introduction

Rutin (3, 4, 5, 7-tetra hydroxyl flavone 3-d-rutinoside) is a flavonoid glycoside compound, widely present in plant sources such as leaves, fruits, and vegetables. It is thought to be an activating factor for Vitamin C and is popularly known as Vitamin P [1]. Rutin is reported to exhibit a broad range of physiological functions such as an anti-inflammatory, anti-tumor, anti-aging, anti-bacterial, anti-oxidant, and hemostatic agent. It is often used as a therapeutic drug against a wide range of circulatory problems as it is proved to dilute the blood, reduce capillary permeability, and lower blood pressure [1–3]. From this perspective, administering the rutin levels in drug tablets, food supplements, and nutraceutical inputs to the patients plays a vital role. Therefore, it is necessary to develop simple, fast, economical, sensitive, and efficient methods for the detection and quantification of rutin in pharmaceutical, food, and nutraceutical samples.

A variety of analytical methods such as UV–Vis spectrophotometry, high-performance liquid chromatography, flow injection analysis, capillary electrophoresis, chemiluminescence, and sequential injection analysis have been developed for the determination of rutin [4–9]. However,

from the pragmatic point of view, these methods suffer from various limitations as they involve complicated operations, expensive instruments, toxic organic solvents, and lengthy separation protocols [3]. Compared to the above methods, electrochemical methods offer several advantages such as high sensitivity, selectivity, wide detection range, simple and speedy procedure, relatively low cost, and feasible onsite monitoring [1, 3]. However, the efficacy of the analyte detection in electrochemical methods is entirely governed by the sensor architecture and the characteristics of sensing materials employed. Rutin exhibits electroactive behavior owing to the presence of flavonoid glycoside group in its structure and is prone to either oxidation or reduction on different working electrodes. Hence rutin can be investigated by electrochemical sensing methods [3].

A variety of carbon-based nanostructures have displayed next-generation potential sensing materials because of their high specific surface area, high-quality crystal lattices, high carrier mobility with superior modifiable conductivity, and the possible ultra-thin film processing options [10, 11]. Among the carbon-based nanomaterials, GNR is a recent member of this family with a quasi-one-dimensional graphene-like structure having narrower widths, exhibiting

semiconductive behavior, quantum confinement, and edge effects. Unlike graphene, GNRs possess a completely different set of properties, such as a large aspect ratio (i.e., the ratio of length to width) and an open band gap that can be controlled by tuning atomic-scale structures. The width of GNRs ranges from sub-10 nm to several hundred nanometers, while the thickness is about several nanometers [12–15]. The surfaces of GNRs are chemically inert and interact with other molecules via physical adsorption (interactions) similar to graphene. GNRs have the densest and most abundant edge defect sites with superior chemical reactivity within a single-channel unit. The narrow channel width of GNRs makes them more accessible to doping and chemical modification [12, 14, 16]. The properties of GNR are dependent on edge type and several chemical groups such as carboxyl (–COOH), carbonyl (–CO), hydrogenated (–CH), and amines (–NH₂), which could be anchored at the edges of GNRs [17]. These characteristics of GNR make it a more promising sensing material compared to graphene. However, due to their recentness of discovery, GNR is not much familiar among the research fraternity, and they are very less explored in sensing applications compared to graphene.

GNR reconciles as novel and excellent material for electrochemistry due to its conductivity, high reactive surface area, and wider electrochemical window. This material shows a large electrochemical potential window (approximately 2.5 V in 0.1 mM phosphate buffer saline solution) in the detection of analytes with either high oxidation or reduction potential becoming feasible [18]. Further, the extremely high surface area provides an effective reaction area and a high capacity for enzyme loading. The presence of abundant edges and defects on this material provides a high electron transfer rate, suggesting that it is suitable for electrochemical detection. The chemical moieties (hydroxy and carboxyl groups) on the GNR surface afford flexibility and convenience for functionalization, which provides a way for enhancing sensor performance [17, 18]. The above characteristics make GNR as a novel material and efficient platform for sensing applications.

The oxidized and reduced forms of GNRs have been reported as sensor electrode material for the detection of glucose, ascorbic acid, L-DOPA, and uric acid in standard samples [14, 19–21]. The sensor developed using reduced GNRs on screen-printed platforms showed improved performance than those developed using carbon paste electrode, MWCNTs, and oxidized GNR [14]. Enzevae et al. [20] modeled and investigated CO₂ adsorption effects on GNR conductance and concluded that the GNRs could be used for the development of the CO₂ gas sensor. GNRs have also been used in the development of non-enzymatic electrochemical glucose sensors [21]. Recently, Cho et al. [13] studied the NO₂ gas sensing potentials of aminopropyl

silane-functionalized GNRs and demonstrated a far superior sensing performance as compared to carbon nanotube and reduced graphene oxide sensors prepared under identical conditions. However, the biosensing applications of GNRs have not been explored much to their full potential as this material is relatively new. The GNR-based rutin sensors are not reported to date to the best of our knowledge and this was the motivation for our work.

In the current work, GNRs derived from longitudinal unzipping of MWCNTs have been employed for the first time in the development of a binder-free, non-enzymatic electrochemical sensor for the determination of rutin.

2 Experimental methods

2.1 Materials and instruments

MWCNTs and potassium permanganate (KMnO₄) were procured from Sigma-Aldrich. Potassium chloride, mono-sodium hydrogen phosphate, disodium hydrogen phosphate, and the reagents sulfuric acid and hydrogen peroxide used in this study were purchased from Fischer Scientific.

All electrochemical experiments such as cyclic voltammetry (CV), differential pulse voltammetry (DPV), and electrochemical impedance spectroscopy (EIS) were performed on an electrochemical workstation (Biologic Science Instrument, Model SP-150).

2.2 Synthesis of GNRs from MWCNTs

The GNRs were synthesized using a protocol already described in the literature [15, 22]. The synthesis involved chemical unzipping of MWCNTs via a two-step chemical oxidation and reduction process. For the synthesis, 300 mg of MWCNTs were mixed with 120 mL of conc. H₂SO₄ (98%) and stirred for 24 h at room temperature till a slurry was obtained. The slurry was later coupled with 1.5 g of KMnO₄ slowly under vigorous stirring conditions and the mixture was further heated for 4 h at 85 °C. The resulted slurry was later diluted by adding 400 mL of deionized water and again kept for stirring in an ice bath for 30 min. After removal from the ice bath, 60 mL of hydrogen peroxide (30%) was added to it followed by the addition of 200 mL of deionized water to avoid the formation of an insoluble precipitate of MnO₂. The cold mixture was washed and centrifuged with 10% HCl and then with deionized water until the solution attains neutral pH. Finally, the resulting solid residue was washed repeatedly with ethanol and deionized water and later dried at 60 °C in vacuum to get dark gray-colored solid powder of GNRs.

The as-synthesized GNRs were characterized by X-ray diffraction (XRD), Fourier transform infrared (FT-IR), and

Raman spectroscopy methods. The morphological studies were carried out by high-resolution tunneling electron microscopy (HR-TEM) method.

2.3 Fabrication of Gr/GNRs sensor

Graphite rod (0.6 mm diameter) was used for the fabrication of the working electrode. The tip of the graphite rod was first polished using PK3 electrode kit till a mirror shiny surface was obtained and the graphite rod was cleaned in ultrapure water and dried. The clean polished graphite rod was then covered with Teflon tube leaving only the polished surface exposed. The resulting graphite electrode (Gr) was cleaned again with distilled water, dried at room temperature, and used for further investigations. A suspension of GNRs was prepared in ultrapure water by dispersing 1.25 g L^{-1} of GNRs powder in distilled water followed by bath sonication for 15 min at room temperature. The appropriate volumes of above GNRs suspension was drop cast on Gr electrode and dried under ambient conditions to get modified Gr/GNRs electrode.

2.4 Electrochemical investigations

All electrochemical investigations including CV, DPV, and EIS were performed in a three-electrode cell comprising of modified Gr (working electrode), saturated calomel electrode (SCE, reference), and platinum wire (counter electrode). All CV studies were executed in PBS under pH 7.0 in the potential window of -0.2 to $+0.6 \text{ V}$. The EIS measurements were performed under similar conditions using $5 \text{ mM} [\text{Fe}(\text{CN})_6]^{3-/4-}$ as an electrochemical probe in the frequency range of 100 kHz to 0.1 Hz . DPV studies were carried out in PBS medium (pH 7.0) by adding known quantities of rutin in the potential window of 0 to $+0.5 \text{ V}$, a pulse amplitude of 25 mV , and pulse width of 50 s .

3 Results and discussions

3.1 Characterization of synthesized GNRs

The successful synthesis of GNRs by chemical unzipping MWCNTs was confirmed through XRD, Raman, and HR-TEM studies. HR-TEM images in Fig. 1a and b display morphological features of MWCNTs and GNRs, respectively. Unlike MWCNTs, which displays smooth and undamaged tubular surface, the GNRs reveal a two-dimensional off-plane deformed and wrinkled ribbon-like 2D structures. These images serve as a preliminary evidence for the successful unzipping of MWCNTs. This evidence was further supported by the results of XRD and Raman analysis.

The XRD profile (Fig. 1c) of GNRs shows two peaks at 2θ values 27° and 45° which is characteristic of GNRs. MWCNTs show only one XRD signal at 27° and this is explicitly indicative of unzipping of MWCNT as evident from the literature [15, 22]. The Raman spectra of GNRs (Fig. 1d) show an enhanced G and D bands with an increased intensity ratio ($I_D/I_G = 1.4$) compared to that of MWCNTs ($I_D/I_G = 1.08$). The higher I_D/I_G ratio of GNRs manifests the higher order of damages and deformations on GNRs surface. The XRD and Raman data provide strong evidence of high-density edge states on GNRs surface in comparison to MWCNTs. The results clearly suggest the successful unzipping of MWCNTs.

3.2 Sensor fabrication and electrochemical characterization

The fabrication of Gr/GNRs was done by depositing different quantities of GNRs stock suspensions (1.25 g L^{-1}) onto the clean Gr electrode. The Gr/GNRs electrodes were prepared by drop-casting GNRs suspensions of 0 , 0.5 , 1.0 , 3.0 , and $5.0 \mu\text{L}$ on to bare Gr electrode surface and air-dried at room temperature. The successful deposition and modification of electrodes were confirmed by electrochemical characterization using the CV technique by measuring the current response in 0.1 mM PBS (pH 7.0). It was observed that the current response increased as the deposition quantity was increased and a stable current response was recorded for all depositions above $1 \mu\text{L}$ (Fig. 2a). Thus, a deposition volume of $1 \mu\text{L}$ GNRs stock solution was used for all later investigations. The improved current at higher deposition volume of GNRs suspensions establishes the conductive nature of GNRs.

Electrochemical redox behavior of Gr and Gr/GNRs electrodes was investigated by CV in the presence of $5 \text{ mM} [\text{Fe}(\text{CN})_6]^{3-/4-}$ as redox mediator in 0.1 mM PBS (pH 7.0). The CV experimental results manifest redox behavior for both bare and GNRs-modified electrodes. However, GNRs-modified electrode showed excellent redox behavior compared to bare Gr electrode with a pair of well-defined quasi-reversible redox peaks (Fig. 2b) and a higher peak current was evident compared to that of the bare Gr electrode. The ascended oxidation and reduction peaks in the CV profile of the modified electrode affirm the exhibition of redox behavior by GNRs-modified electrodes. The enhanced peak currents recorded for modified electrodes in the presence of the redox mediator is closely linked to the conductive nature of GNRs and also the active surface coverage area of the electrodes. The active surface area (τ) of both Gr and Gr/GNRs electrodes were calculated using the equation [22];

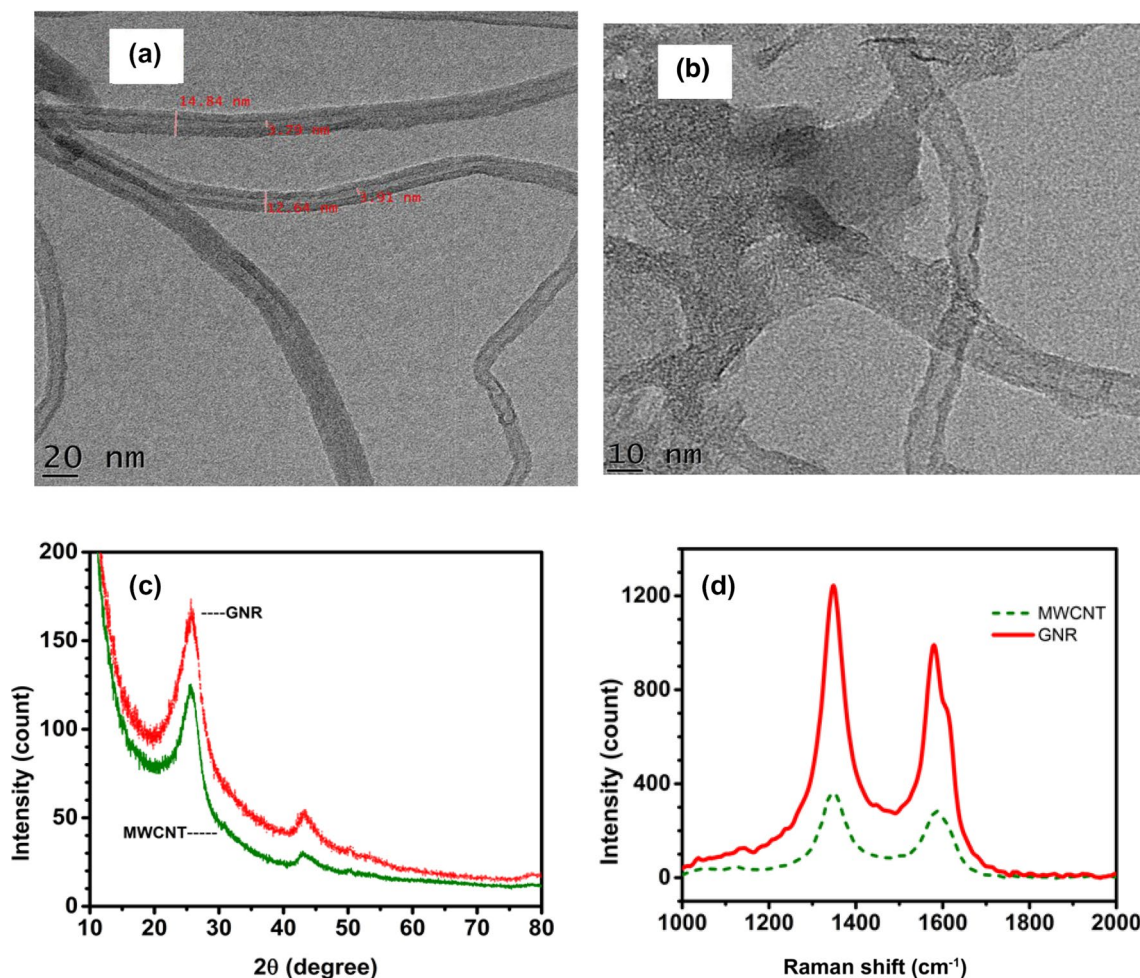


Fig. 1 **a** HR-TEM image of MWCNT and **b** GNRs, XRD (**c**), and Raman (**d**) profiles of MWCNT and GNRs

$$\tau = \frac{Q}{nFA},$$

where Q is the charge, n is the number of electrons transferred, F is the Faraday constant, and A is the geometric area of the working electrode. The calculated active surface area of the Gr and Gr/GNRs electrodes was $1.268 \times 10^{-10} \text{ mol cm}^{-2}$ and $1.817 \times 10^{-8} \text{ mol cm}^{-2}$, respectively. The active electrode surface coverage area was enhanced nearly 100 times on the deposition of GNRs to the Gr electrode surface which assures increased catalytic activity on the Gr/GNRs electrode surface. This envisages the enhanced current response of the Gr/GNRs electrode compared to the Gr electrode in the presence of redox mediator. The electrochemical behavior of rutin was investigated by CV in PBS (0.1 mM, pH 7.0) by adding 1 mM rutin (Fig. 2c). The recorded current response was higher for Gr/GNRs with rutin compared to the responses of both Gr and Gr/GNR

electrodes in the presence of PBS (0.1 mM, pH 7.0). This clearly establishes the exhibition of good electrocatalytic behavior of electrode towards rutin.

The CV results were further validated by conducting EIS experiments under the same experimental conditions in the frequency range of 100 kHz to 10 MHz with an amplitude of 5 mV. The obtained EIS experimental data are represented in the Nyquist plot (Fig. 2d) and the data were also fitted to an equivalent circuit given in the inset of Fig. 2d. Table 1 represents the various impedance parameters such as solution resistance (R_s), Faraday capacitance charge transfer (Q_{dl}), charge transfer resistance (R_{ct}), Faraday capacitance (C_f), Faraday resistance (R_f), and the number of electrons exchanged (n). The calculated R_{ct} values for bare and GNRs-modified electrodes based on the equivalent circuit are $76.1 \Omega \text{ cm}^{-2}$ and $47.4 \Omega \text{ cm}^{-2}$, respectively. The observed reduction in R_{ct} values of Gr/GNRs show enhancement in the conductivity of electrodes due to the enhanced surface

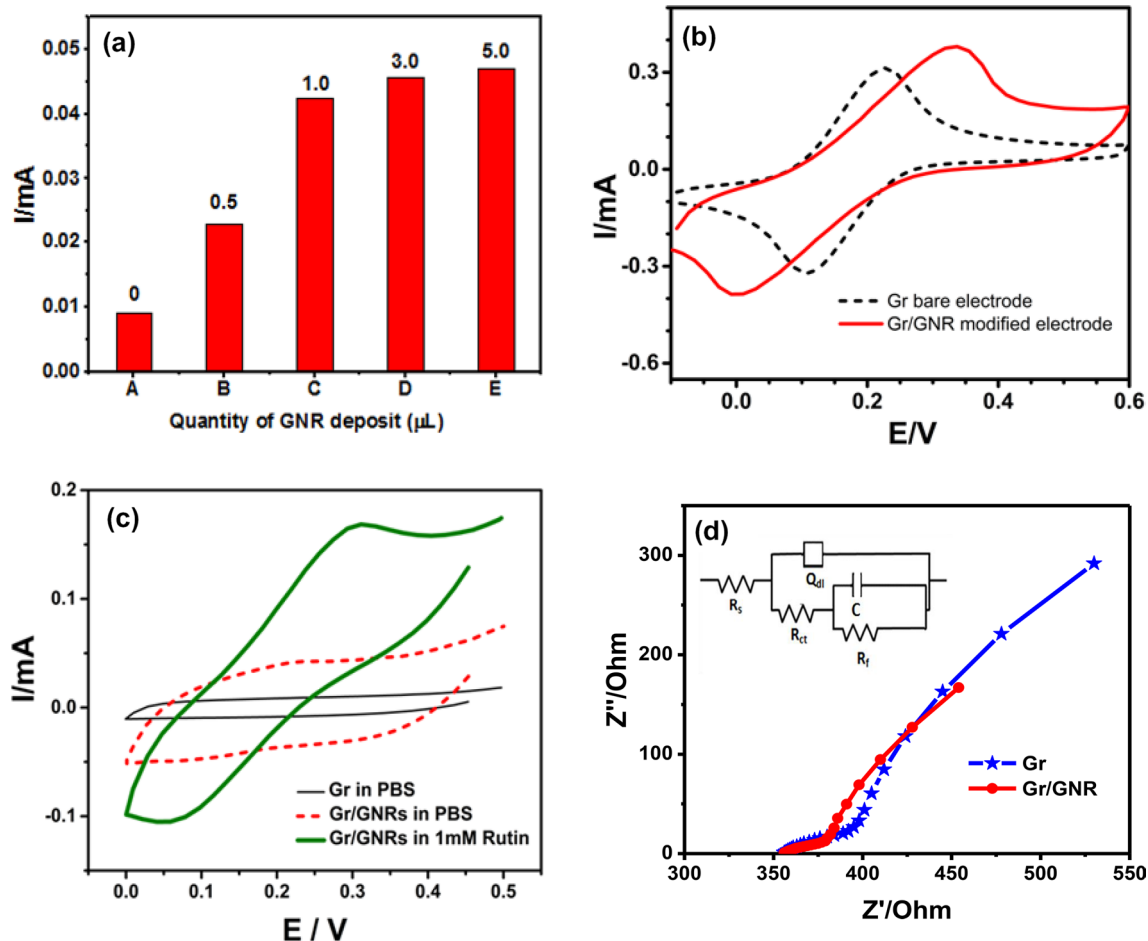


Fig. 2 **a** Current response of Gr at different depositions of GNR. **b** CVs of 5 mM $\text{Fe}(\text{CN})_6^{3-/4-}$ solution obtained at (a) Bare Gr and (b) Gr/GNRs, **c** CVs recorded in 0.1 M PBS at (a) Bare Gr, (b) Gr/GNR,

and (c) Gr/GNRs in presence of 1 mM rutin, and **d** impedance spectrum of (a) Bare Gr, (b) Gr/GNRs

Table 1 Equivalent circuit parameters of bare and GNR-modified Gr electrodes

Electrode	R_s ($\Omega \text{ cm}^{-2}$)	Q_{dl}	R_{ct} ($\Omega \text{ cm}^{-2}$)	n	C_f	R_f ($\Omega \text{ cm}^{-2}$)
Gr	355.5	1.99×10^{-3}	76.1	0.57	2.29×10^{-3}	2.40×10^3
Gr/GNR	355.6	4.12×10^{-3}	47.4	0.48	3.47×10^{-3}	9.72×10^3

area. Moreover, Nyquist plots of bare and modified Gr electrode reveal an enlarged semi-circular region with a higher diameter for the Gr electrode compared to GNRs-modified electrode indicating a higher charge transfer resistance for the Gr electrode. These results show concurrence with those of CV. The remarkable increase in current response could be attributed to the larger surface area and also creation of active sites provided by GNRs which accelerate electron transfer behavior at the electrode/electrolytes interface, thus producing an amplified electrochemical signal.

3.3 Effect of scan rate

The scan rate is a vital parameter in deciding the electrochemical response of a sensor. The effect of scan rate on electrochemical response of the Gr/GNRs sensor was probed at different scan rates from 20 to 120 mV s^{-1} by CV method taking 2 mM rutin in PBS (0.1 M, pH 7.0). The voltammogram of CV data showed a pair of well-defined redox peaks whose peak currents gradually increased with an increase in scan rate (Fig. 3a). The plots between anodic peak current (I_a) and scan rate (\sqrt{v}), and anodic peak current (I_a) versus square root of scan rate ($\sqrt{v/2}$), are drawn and shown as Fig. 3b and c, respectively. The

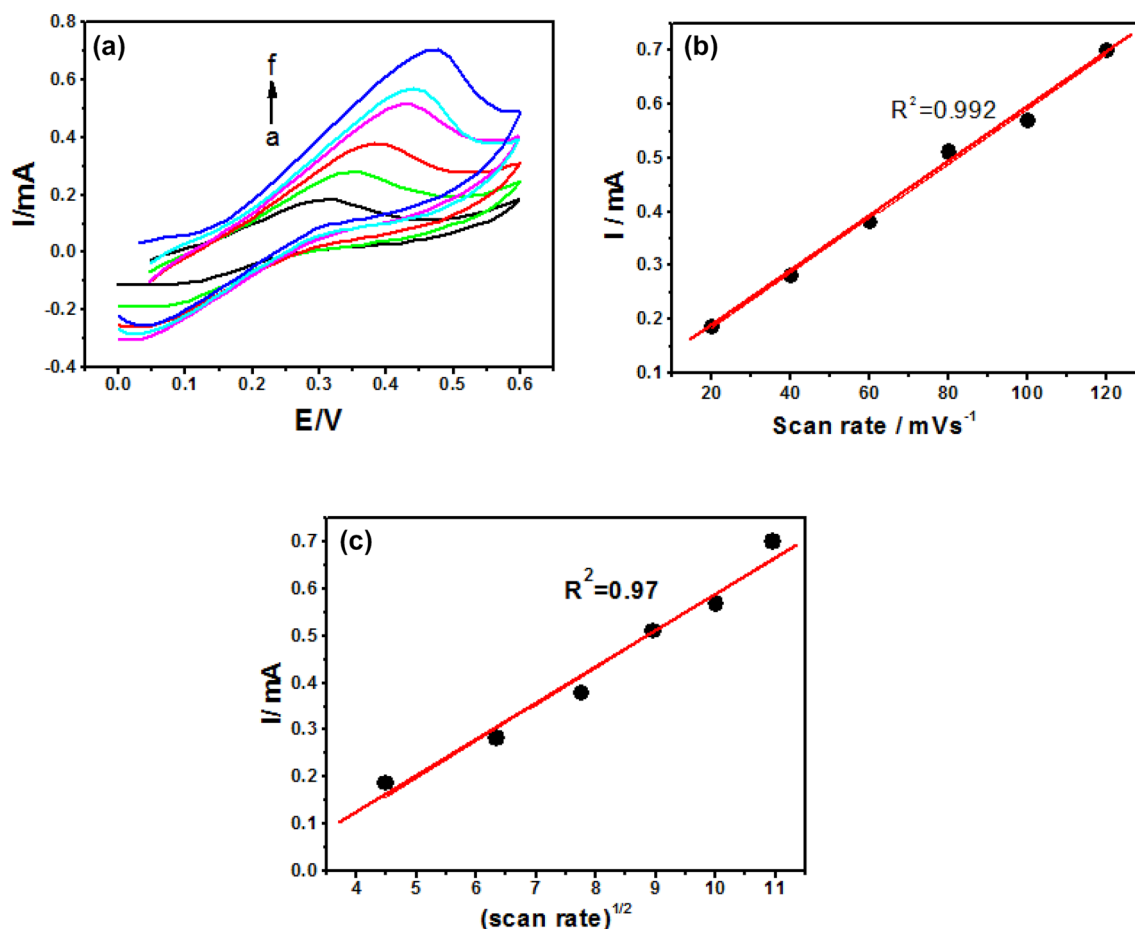


Fig. 3 a Cyclic voltammograms of Gr/GNRs in 0.1 M PBS (pH 7) containing 2 mM rutin at different scan rate (a–f), b plots of peak current vs. scan rate, and c peak current vs. square root of scan rate

relation between peak current and scan rate (ν) showed a linear dependence with a linear regression co-efficient $R^2 = 0.992$, whereas the relationship between peak current versus square root of scan rate ($\sqrt{\nu}$) also showed a linear relationship with a regression co-efficient $R^2 = 0.97$. The corresponding regression relations are,

$$I = (0.0051)\nu + 0.083; R^2 = 0.99,$$

$$I = (0.0785)\sqrt{\nu} + 0.1948; R^2 = 0.97.$$

This suggested linearity of sensor response implies that the electrode reaction of rutin at the electrode surface is predominantly a diffusion-controlled adsorption process.

3.4 Electrochemical determination of rutin on Gr/GNRs

DPV is a voltammetric technique that offers high sensitivity and selectivity in the electrochemical determinations for

low analyte concentrations. The DPV response obtained for different rutin concentrations ranging from 32 to 1000 nM in PBS (0.1 M) under optimized experimental conditions (pH 7.0, pulse width 50 s, pulse height 25 mV) is shown in Fig. 4a. The voltammetric response varied linearly exhibiting two distinct concentration regimes viz., 32–100 nM and 100–1000 nM with regression coefficients $R^2 = 0.8964$ and 0.991, respectively.

The mechanism of electro-oxidation of rutin is well documented in the literature [23]. The mechanism involves the ionization of *ortho*-phenolic hydroxyl group followed by one-electron oxidation of monoanionic species to form an intermediate radical anion. Later, the radical anion undergoes a second reversible one-electron oxidation to give dehydrorutin which rapidly protonates and dehydrates to yield 3',4'-diquinone as the final product. The conversion of rutin to quinine or vice versa during electrode reactions is detected through measurement of oxidation/reduction currents during the redox reactions at the electrode surface. The

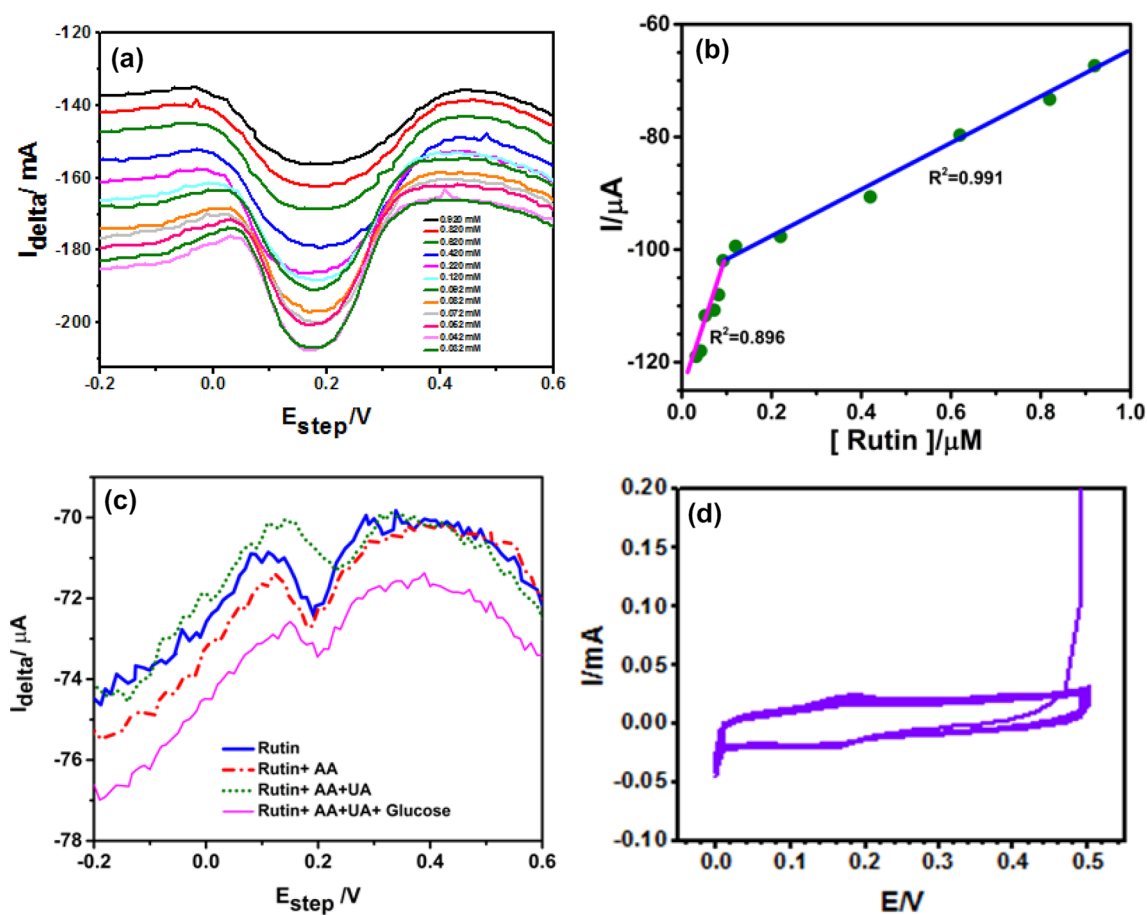
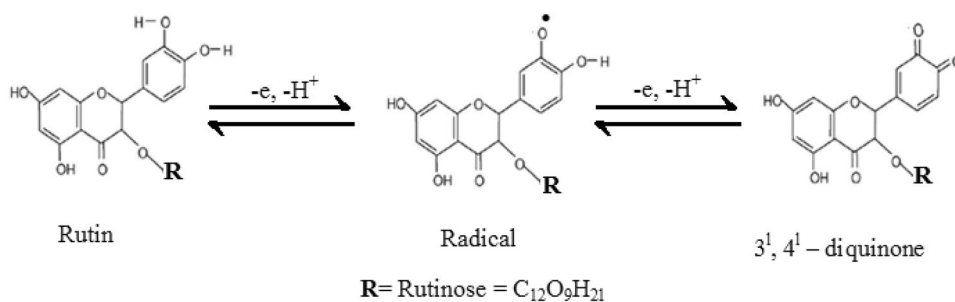


Fig. 4 **a** DPVs of Gr/GNRs electrode at varying rutin concentration 32–1000 nM in 0.1 M PBS solution. **b** Plot shows calibration plot of peak current versus catechol concentration for DPV data. **c** Effect of

presence of interferences AA, UA, and glucose on current response of sensor in 1 mM rutin. **d** Stability of sensor response observed for 20 cycles in 5 μM rutin

Scheme 1 Mechanism of electro-oxidation of rutin to quinone



detailed mechanism of action of electro-oxidation of rutin on the electrode surface is shown in Scheme 1.

3.5 Detection limit and sensitivity of sensor

The detection limit (LOD) and sensitivity were calculated using the following equations [24];

$$\text{LOD} = \frac{3\sigma}{\theta},$$

$$\text{Sensitivity} = \frac{\theta}{A},$$

where σ is the standard deviation of blank, θ is the slope of the calibration plot, and A is the surface area of the electrode (Fig. 4b). The LOD calculated based on signal-to-noise ratio ($S/N=3$) is 7.862 nM and sensitivity is 917.23 $\mu\text{A } \mu\text{M}^{-1} \text{ cm}^{-2}$ for the concentration region 32–1000 nM. These results suggest that the developed GNRs-based rutin sensor offers a reasonable linear range, excellent detection

Table 2 Comparison of proposed sensor with previously reported sensors

Sensor matrix used	Method employed	Linear range (nM)	Detection limit (nM)	References
GCE/GN	DPV	100–10,000	21	[25]
GCE/ErGO	DPV	470–12,500	18.4	[26]
GCE/ErGO-Fe ₃ O ₄ -NH ₂	SDLV	6–100	4	[27]
GCE/MWCNT@rGO@Pt	DPV	50–50,000	5	[28]
GCE/PdPc-MWCNT	Amperometry	100–51,000	75	[29]
Gr/GNR	DPV	32–100	7.86	Present work

GCE glassy carbon electrode, GN graphene nanosheet, ErGO electrically reduced graphene oxide, Pt platinum, PdPc palladium-decorated phthalocyanine

limit, and high sensitivity owing to the good conductivity, high surface area, and also synergic effects offered by carbon nanotube-derived GNRs. This suggests that the Gr/GNR is a promising electrode material for sensitive detection of rutin.

The performance of the proposed sensor was compared with some previously reported sensors for rutin analysis, and their analytical parameters are summarized in Table 2. As enlisted in Table 2, the proposed sensor shows a reasonable linear analytical range and detection limit comparable to (even superior to) other sensors. Besides, the proposed fabrication procedure is simple and time-saving being a single-step process.

3.6 Selectivity, repeatability, and stability studies

The interference and selectivity study of the sensor towards rutin was investigated under optimized experimental conditions by DPV technique using 1 mM rutin in the presence and absence of common interferents such as uric acid (UA), ascorbic acid (AA), and glucose. The AA (0.01 mM), UA (0.01 mM), and glucose (0.01 mM) were introduced to 1 mM rutin in successive steps and the current response was recorded in 0.1 M PBS (pH 7.0). The measured current responses of the sensor for 1 mM rutin in the presence of different interferents were not much different from the response recorded in the absence of interferents. The observed change in current response was well below 2% suggesting that the Gr/GNRs sensor showed excellent selectivity to rutin. The DPV results of interference studies are shown in Fig. 4c and the data are given in Supplementary File S1.

The intra-electrode repeatability of rutin sensor was investigated with a series of repetitive measurements in 1 mM rutin under optimized experimental conditions. The sensor showed no significant changes in response (RSD < 3%) suggesting good repeatability of the sensor. The stability of rutin sensor was also examined by monitoring the CV response of the sensor for 20 redox cycles in presence of 5 μM rutin (Fig. 4d) and it was observed that the sensor retained nearly 98% of its initial response thereby depicting high chemical stability for the sensor matrix.

3.7 Practical application of sensor

The practical applicability of the fabricated sensor was used to analyze rutin drug tablets. A known weight of commercially available rutin drug tablet sample (500 mg rutin/tablet, Lupin India Ltd.) was ground and dissolved in ethanol and standard rutin solution was prepared. The analysis of the sample solution was performed under optimized experimental conditions by introducing it into the electrochemical cell containing 0.1 M PBS (pH 7.0) and bovine serum. The results from these measurements showed an excellent recovery in the range of 96.25–102% indicating that the proposed sensor could be efficiently applied in the determination of rutin in real samples with good accuracy (Table 3).

4 Conclusion

A binder-free non-enzymatic electrochemical sensor based on GNRs was developed for the sensitive and selective determination of rutin. The GNRs were synthesized by a simple procedure involving chemical unzipping of MWCNTs in an oxidative environment and the as-prepared GNRs were further employed in development of rutin sensor. The fabrication of the sensor was accomplished by modifying the Gr electrode with optimized quantity of GNRs. The modification with GNRs was found to enhance the active surface area of the electrode nearly 100 folds which is further revealed in enhanced electrocatalytic activity of the electrode. This clearly suggests that the GNRs play dual role in the electrode matrix both as a conductor and also as an

Table 3 Recovery results of rutin tablet analysis in bovine serum medium

No	Rutin added (nM)	Rutin found (nM)	Percentage recovery
1	40	38.5	96.25
2	100	102	102.0

excellent electro-catalyst. GNRs not only showed good electrocatalytic behavior but also imparted needed stability for the electron transfer at the electrode–electrolyte interface. The sensor showed excellent electrocatalytic activity, good stability, repeatability, and high selectivity towards rutin. The detection limit and sensitivity were found to be 7.86 nM and 917.2 $\mu\text{A } \mu\text{M}^{-1} \text{ cm}^{-2}$, respectively. This excellent performance is solely attributed to the large surface area, good conductivity, and strong electrocatalytic behavior of GNRs. The simple sensor configuration, simplicity of fabrication procedure, no need of any binding agent, or enzyme in fabrication process coupled with good electrochemical performance make this sensor a strong candidate in the electroanalysis of rutin samples from food, pharmaceutical, and nutraceutical industries.

Supplementary Information The online version contains supplementary material available at <https://doi.org/10.1007/s10800-021-01557-x>.

Acknowledgements One of the first authors gratefully acknowledge the encouragement and partial financial support received from the management of Sri Jayachamarajendra College of Engineering, JSS Science and Technology University, Mysuru, Karnataka, India, during this research work.

Author contributions NKS: Investigation and Writing—original draft. KNSM: Review and editing and Supervision. MBH: Methodology. AMM: Resources. SRN: Validation. KR: Resources.

Declarations

Conflict of interest There is no conflict of interest in this paper.

References

- Yang X, Long J, Sun D (2016) Highly-sensitive electrochemical determination of rutin using NMP-exfoliated graphene nanosheets-modified electrode. *Electroanalysis* 28:83–87. <https://doi.org/10.1002/elan.201500449>
- Guo R, Wei P (2008) Studies on the antioxidant effect of rutin in the microenvironment of cationic micelles. *Microchim Acta* 161:233–239. <https://doi.org/10.1007/s00604-007-0888-7>
- Pang P, Li H, Liu Y, Zhang Y, Feng L, Wang H, Wu Z, Yang W (2015) One-pot facile synthesis of platinum nanoparticle decorated reduced graphene oxide composites and their application in electrochemical detection of rutin. *Anal Methods* 7:3581–3586. <https://doi.org/10.1039/c5ay00353a>
- Hassan HNA, Barsoum BN, Habib IHI (1999) Simultaneous spectrophotometric determination of rutin, quercetin and ascorbic acid in drugs using a Kalman Filter Approach. *J Pharm Biomed Anal* 20:315–320. [https://doi.org/10.1016/s0731-7085\(99\)00048-5](https://doi.org/10.1016/s0731-7085(99)00048-5)
- Santagati N, Salerno AL, Attaguile G, Savoca F, Ronsisvalle G (2008) Simultaneous determination of catechins, rutin, and gallic acid in *Cistus* species extracts by HPLC with diode array detection. *J Chromatogr Sci* 46:150–156. <https://doi.org/10.1093/chromsci/46.2.150>
- Yang D, Li H, Li Z, Hao Z, Li J (2010) Determination of rutin by flow injection chemiluminescence method using the reaction of luminol and potassium hexacyanoferrate(III) with the aid of response surface methodology. *Luminescence* 25(6):436–444. <https://doi.org/10.1002/bio.1172>
- Deng PH, Xu ZF, Feng YL (2012) Highly sensitive and simultaneous determination of ascorbic acid and rutin at an acetylene black paste electrode coated with cetyltrimethyl ammonium bromide film. *J Electroanal Chem* 683:47–54. <https://doi.org/10.1016/j.jelechem.2012.08.002>
- Xu H, Li Y, Tang HW, Liu CM, Wu QS (2010) Determination of rutin with UV–Vis spectrophotometric and laser-induced fluorimetric detections using a non-scanning spectrometer. *Anal Lett* 43:893–904. <https://doi.org/10.1080/00032710903488795>
- Legnerova Z, Satinsky D, Solich P (2003) Using on-line solid phase extraction for simultaneous determination of ascorbic acid and rutin trihydrate by sequential injection analysis. *Anal Chim Acta* 497:165–174. <https://doi.org/10.1016/j.aca.2003.07.007>
- Llobet E (2013) Gas sensors using carbon nanomaterials: a review. *Sens Actuators B* 179:32–45. <https://doi.org/10.1016/j.snb.2012.11.014>
- Sandeep S, Santhosh AS, Swamy NK, Suresh GS, Melo JS, Nithin KS (2018) Electrochemical detection of L-DOPA using crude polyphenol oxidase enzyme immobilized on electrochemically reduced rGO–Ag nanocomposite modified graphite electrode. *Mater Sci Eng B* 232–235:15–21. <https://doi.org/10.1016/j.mseb.2018.10.014>
- Huang B, Li Z, Liu Z, Zhou G, Hao S, Wu J, Gu B-L, Duan W (2008) Adsorption of gas molecules on graphene nanoribbons and its implication for nanoscale molecule sensor. *J Phys Chem C* 112:13442–13446. <https://doi.org/10.1021/jp8021024>
- Cho KM, Cho SY, Chong S, Koh H-J, Kim DW, Kim J, Jung H-T (2018) Edge-functionalized graphene nanoribbon chemical sensor: comparison with carbon nanotube and graphene. *ACS Appl Mater Interfaces* 10:42905–42914. <https://doi.org/10.1021/acsami.8b16688>
- Martín A, Hernández-Ferrer J, Martínez MT, Escarpa A (2015) Graphene nanoribbon-based electrochemical sensors on screen-printed platforms. *Electrochim Acta* 172:2–6. <https://doi.org/10.1016/j.electacta.2014.11.090>
- Kosynkin DV, Higginbotham AL, Sinitskii A, Lomeda JR, Dimiev A, Price BK, Tour JM (2009) Longitudinal unzipping of carbon nanotubes to form graphene nanoribbons. *Nature* 458:872–876. <https://doi.org/10.1038/nature07872>
- Wang ZF, Li Q, Zheng H, Ren H, Su H, Shi QW, Chen J (2007) Tuning the electronic structure of graphene nanoribbons through chemical edge modification: a theoretical study. *Phys Rev B* 75:113406. <https://doi.org/10.1103/PhysRevB.75.113406>
- Terrones M, Botello-Méndez AR, Campos-Delgado J, López-Urías F, Vega-Cantú YI, Rodríguez-Maciás FJ, Terrones H (2010) Graphene and graphite nanoribbons: morphology, properties, synthesis, defects and applications. *Nano Today* 5:351–372. <https://doi.org/10.1016/j.nantod.2010.06.010>
- Lin J, Liu Z, Barrow CJ, Yang W (2015) Molecularly engineered graphene surfaces for sensing applications: a review. *Anal Chim Acta* 859:1–19. <https://doi.org/10.1016/j.aca.2014.07.031>
- Jaiswal NK, Kovacevic G, Pivac B (2015) Reconstructed graphene nanoribbon as a sensor for nitrogen based molecules. *Appl Surf Sci* 357:55–59. <https://doi.org/10.1016/j.apsusc.2015.08.219>
- Enzevae A, Akbari E, Buntat Z (2015) Investigation of carbon dioxide adsorption effects on graphene nanoribbon conductance. *Electron Lett* 51:1092–1094. <https://doi.org/10.1049/el.2015.0094>
- Ismail N, Le QH, Yoshikawa H, Saito M (2014) Development of non-enzymatic electrochemical glucose sensor based on graphene oxide nanoribbon–gold nanoparticle hybrid. *Electrochim Acta* 146:98–105. <https://doi.org/10.1016/j.electacta.2014.08.123>
- Sandeep S, Santhosh AS, Swamy NK, Suresh GS, Melo JS, Chamaraja NA (2018) A biosensor based on a graphene

- nanoribbon/silver nanoparticle/polyphenol oxidase composite matrix on a graphite electrode: application in the analysis of catechol in green tea samples. *N J Chem* 42:16620–16629. <https://doi.org/10.1039/C8NJ02325E>
23. Medvidovic-Kosanovic M, Seruga M, Jakobek L, Novak I (2010) Electrochemical and antioxidant properties of rutin. *Collect Czechoslov Chem Commun* 75:547–561. <https://doi.org/10.1135/cccc2009548>
24. Santhosh AS, Sandeep S, Swamy NK, Suresh GS, Melo JS, Chamaraja NA (2019) Fabrication of potentiometric glucose biosensor based on two variant dimensions of green synthesized silver nanostructures as a single nanohybrid compartment—a green approach. *Sens Lett* 17:1–8. <https://doi.org/10.1166/sl.2019.4147>
25. Du H, Ye J, Zhang J, Huang X, Yu C (2010) Graphene nanosheets modified glassy carbon electrode as a highly sensitive and selective voltammetric sensor for rutin. *Electroanalysis* 22:2399–2406. <https://doi.org/10.1002/elan.201000110>
26. Zhang P, Gou Y-Q, Gao X, Bai R-B, Chen W-X, Sun B-L, Hu F-D, Zhao W-H (2016) The pharmacokinetic study of rutin in rat plasma based on an electrochemically reduced graphene oxide modified sensor. *J Pharm Anal* 6:80–86. <https://doi.org/10.1016/j.jpha.2015.12.003>
27. He Q, Wu Y, Tian Y, Li G, Liu J, Deng P, Chen D (2019) Facile electrochemical sensor for nanomolar rutin detection based on magnetite nanoparticles and reduced graphene oxide decorated electrode. *Nanomaterials* 9:115–131. <https://doi.org/10.3390/nano9010115>
28. Tursynbolat S, Bakytkarim Y, Huang J, Wang L (2019) Highly sensitive simultaneous electrochemical determination of myricetin and rutin via solid phase extraction on a ternary Pt@rGO@MWCNTs nanocomposite. *J Pharm Anal* 9:358–366. <https://doi.org/10.1016/j.jpha.2019.03.009>
29. Xing R, Yang H, Li S, Yang J, Zhao X, Wang Q, Liu S, Liu X (2017) A sensitive and reliable rutin electrochemical sensor based on palladium phthalocyanine–MWCNTs–Nafion nanocomposite. *J Solid State Electrochem* 21:1219–1228. <https://doi.org/10.1007/s10008-016-3447-5>

Publisher's Note Springer Nature remains neutral with regard to jurisdictional claims in published maps and institutional affiliations.